

Two vertical bars are positioned on the left side of the page: a thick blue bar on the left and a thinner cyan bar on the right.

NORSAR Scientific Report No. 1-2013

Semiannual Technical Summary

1 January – 30 June 2013

Tormod Kværna (Ed.)

Kjeller, December 2013

6.4 Detection Capability of the Seismic Station TROLL in Antarctica

6.4.1 Introduction

The seismic station at the Norwegian Research Base Troll in Dronning Maud Land, Antarctica, has been operational and sending continuous data to NORSAR since 5 February 2012. The TROLL station (Fig. 6.4.1) is placed on a bedrock prominence on top of a hill, and is equipped with a Streckeisen STS-2.5 broadband seismometer, which can measure ground movements in the frequency range from below 1 mHz up to about 50 Hz. The digitizer is a Quanterra Q330HR, which converts the analog seismometer signals with an over 150db dynamic range (26 bit AD converter) and samples the data streams with rates of 100 Hz, 40 Hz, 1 Hz, 10 s and 100 s (Schweitzer *et al.*, 2012). During the first year of operation, high-quality recordings of both regional and teleseismic signals were made (Pirli, 2012), indicating that the TROLL station would make a significant contribution to seismicity monitoring on both global, regional and local scales.

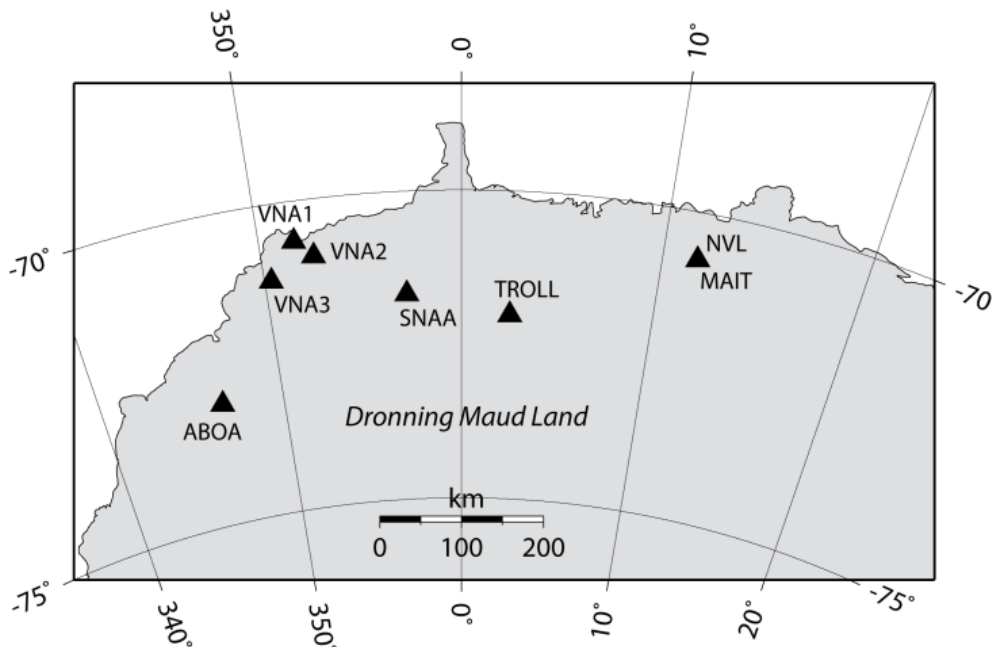


Fig. 6.4.1 Locations of seismic stations in Dronning Maud Land, Antarctica. Seismic data from TROLL, VNA(1-3) and SNAA are accessible in real time.

Figs. 6.4.2 and 6.4.3 show an example of waveforms and corresponding spectra of a PKP-phase recorded at TROLL from a deep earthquake (626 km) located in the Sea of Okhotsk, occurring on 14 August 2012. The event had a magnitude of 7.7 and is located at a distance of 152° from TROLL. Somewhat surprisingly, clear signal energy can be observed well above 10 Hz even at such a large epicentral distance. We also notice from Fig. 6.4.3 that the noise levels at TROLL station stay very close to the Peterson low noise model (Peterson, 1993) for relatively high frequencies, and thus facilitate the observation of small-amplitude high-frequency signals.

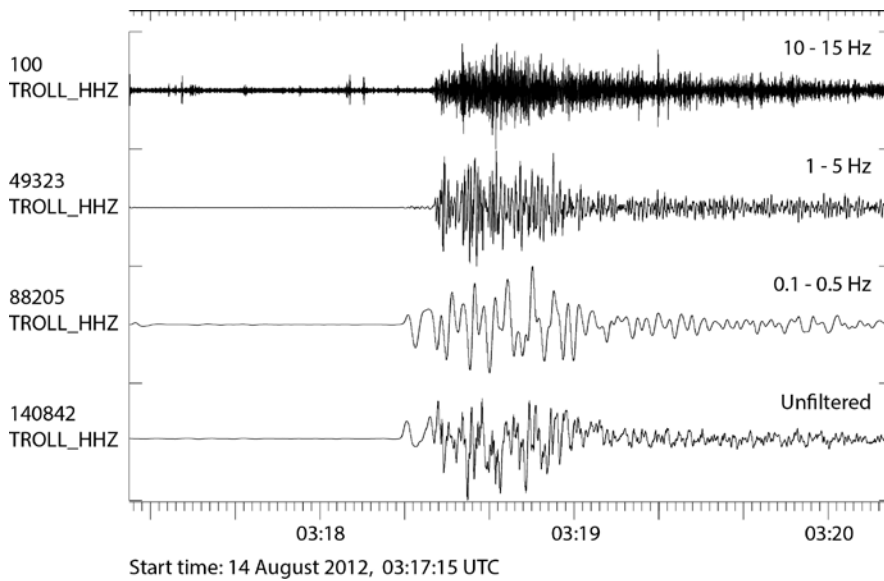


Fig. 6.4.2
PKP-phase from a large deep event in the Sea of Okhotsk recorded at the TROLL station. The event, occurring on 14 August 2012, had a magnitude of 7.7 and was located at a depth of 626 km.

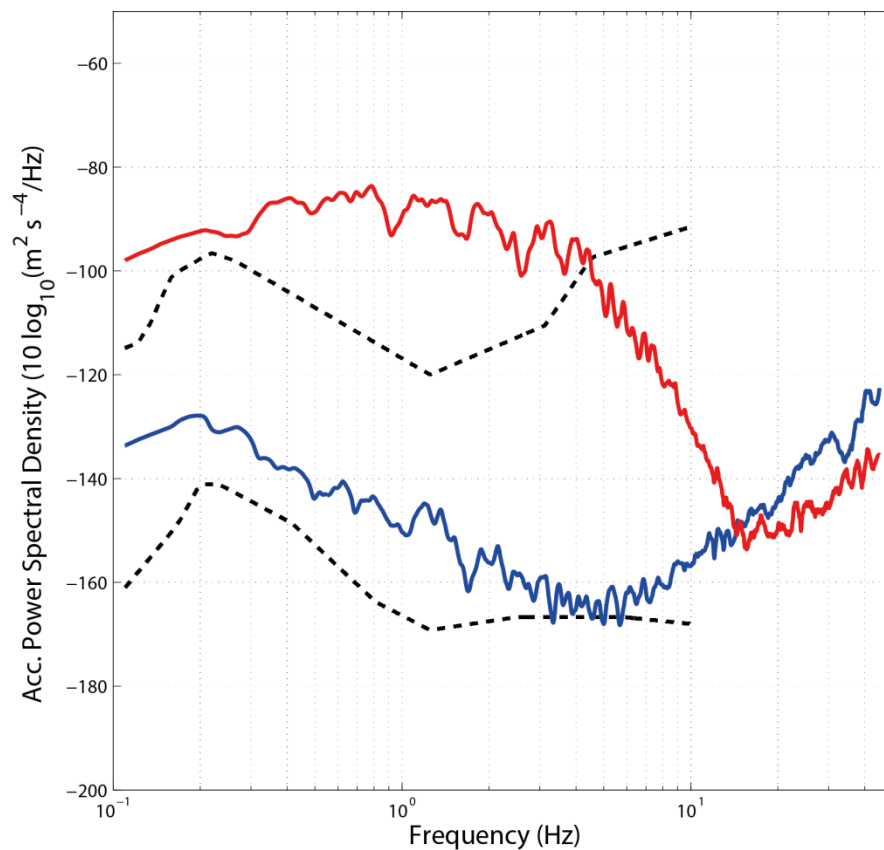


Fig. 6.4.3
TROLL HHZ channel signal acceleration spectrum (red) of the PKP-phase from the Sea of Okhotsk event (see Fig. 6.4.2). A 60 second time segment was used for estimation. The blue curve shows the noise spectrum of a 60 second time window preceding the PKP-phase. The Peterson low- and high-noise models are shown as black dashed lines.

6.4.2 Estimation of detection capability

In the study of Kværna and Ringdal (2013), it was shown that the station SNA in Antarctica was among the best performing three-component stations of the International Monitoring System (IMS) for monitoring compliance with the Comprehensive Nuclear-Test-Ban Treaty (CTBT).

In order to evaluate the performance of the TROLL station, we have made a comparative study with SNAA using IDC Reviewed Bulletin Data (REB) for the time period 5 February 2012 to 13 March 2013. For a noise window preceding the detected REB P-phases, we measured at TROLL and SNAA the long-term average (LTA) amplitude levels in two different frequency bands, 1 – 2 Hz and 2 – 4 Hz. The results are shown in Fig. 6.4.4 and indicate similar noise levels at these two stations. Also notice the annual variation with lower noise levels during the austral winter.

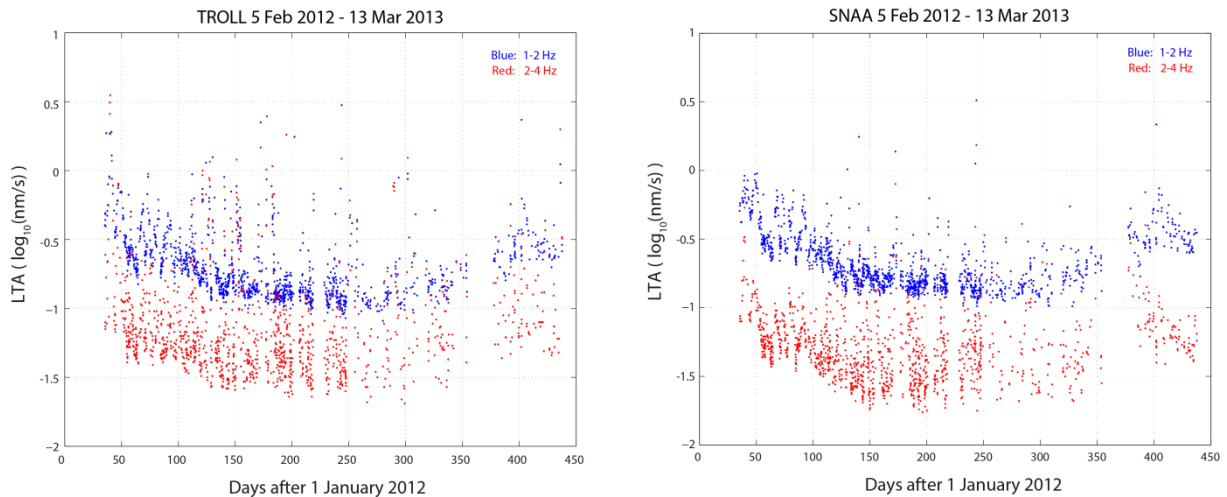


Fig. 6.4.4 Long-term average (LTA) noise levels at TROLL (left) and SNAA (right) during the time period 5 February 2012 to 13 March 2013. The LTAs are calculated in two frequency bands, 1 – 2 Hz and 2 – 4 Hz, for time intervals preceding the P-phases.

For a subset of the REB events, covering the 6-month time period 5 February 2012 to 7 August 2012, we have manually screened the TROLL and SNAA detection lists for REB events having P-detections at both stations. This resulted in a list of 1455 events, shown in Fig. 6.4.5. For both TROLL and SNAA, the P-phases from these events were analyzed in the same manner.

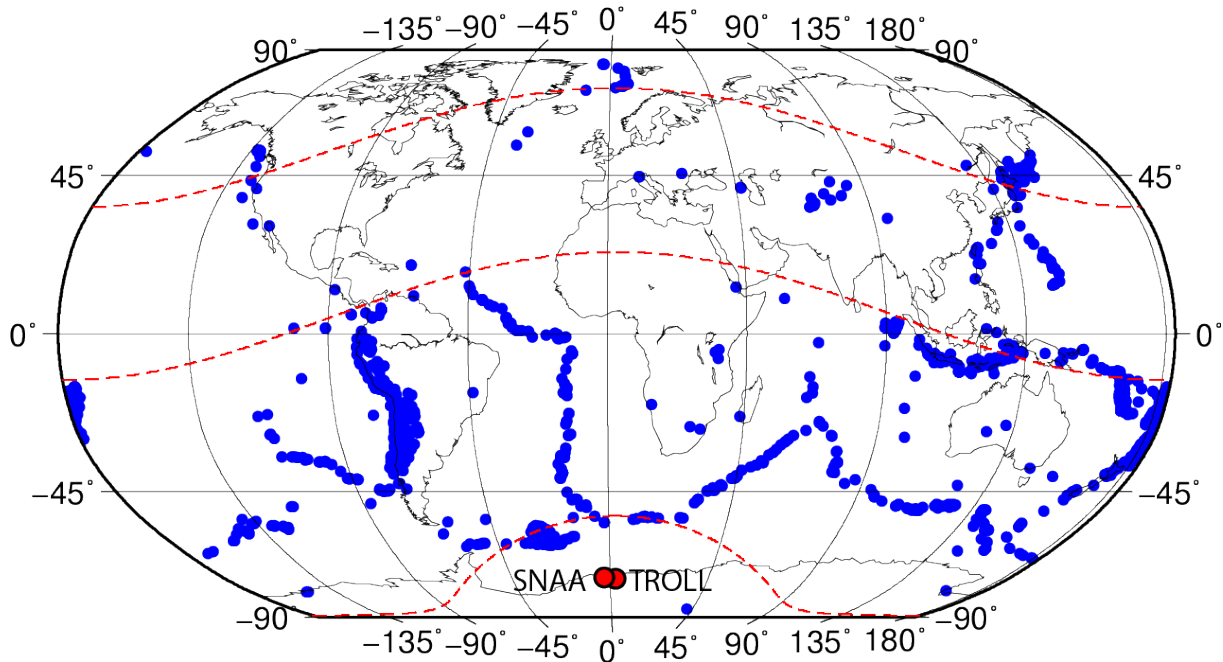


Fig. 6.4.5 Blue symbols show locations 1455 IDC REB events used to estimate the detection capability at the SNAA and TROLL stations. The red dashed curves denote distances of 20, 95 and 144° from TROLL.

To estimate the station detection thresholds, we used a procedure similar to that of Kværna and Ringdal (2013). For each of the events shown in Fig. 6.4.5, we estimated for P-phases at both TROLL and SNAA the instantaneous station detection threshold

$$a_i = m_i - \log(SNR_i) + 0.5$$

where m_i is the reference magnitude (m_{b1}) according to the REB for the i -th event, SNR_i is the signal-to-noise ratio for the i -th event, and the term 0.5 is introduced to take into account the signal-to-noise ratio required for signal detection (0.5 magnitude units correspond to an SNR of ≈ 3). We then fitted the m_{b1} detection capability curve to the instantaneous station detection thresholds, using an average correction (offset) for each of the three distance ranges 0 – 20°, 20 – 90° and 115 – 180°. The results from this analysis are shown in Fig. 6.4.6. The offset is indicative of the overall station performance, and the lower the offset, the better is the overall performance.

From Fig. 6.4.6 we read that for teleseismic distances 20 – 90° and 115 – 180° the offset for TROLL is 0.1 – 0.2 magnitude units lower than for SNAA. Thus, for events in this distance range, TROLL has an overall detection capability which is 0.1 – 0.2 magnitude units better than SNAA. From Fig. 6.4.5, we also see that the sampling of regional events in the distance range 0 – 20° from the two stations is very sparse. The events are limited to very specific areas on the neighboring plate boundaries, like the South Sandwich Islands, and the estimated detection capability from these events may therefore not be very representative for the overall performance within regional distances. However, for the events analyzed, SNAA has a significantly better overall detection capability of 0.5 magnitude units. This may be explained by high frequency noise often observed at TROLL caused by wind and local icequakes (Pirli, 2012). But it is also possible that the propagation path from the geographically clustered regional events to SNAA is particularly favorable in providing strong amplitude signals as

compared with the propagation path to TROLL. Also notice that SNAA is located closer to the regional event cluster than TROLL.

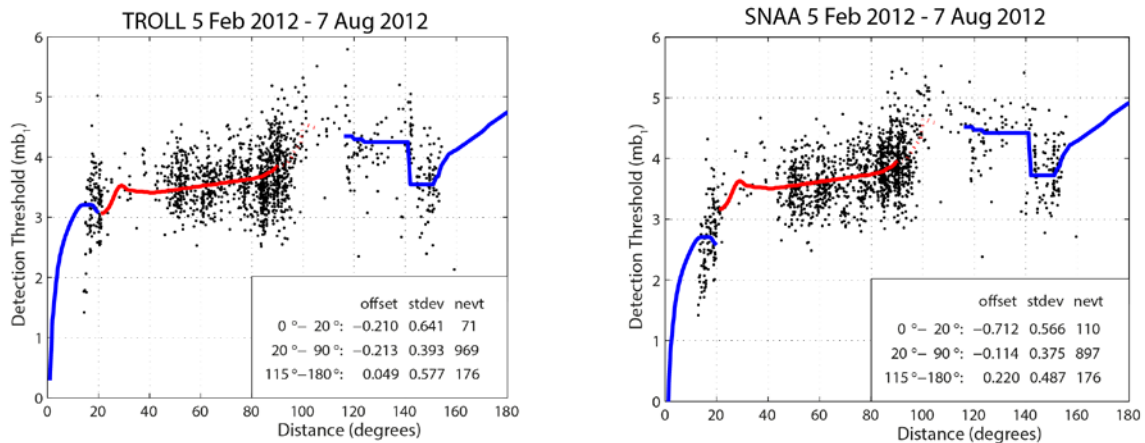


Fig. 6.4.6 The black dots correspond to the estimated instantaneous detection thresholds of the events shown in Fig. 6.4.5., plotted versus the epicentral distance from the stations TROLL (left) and SNAA (right). The standard m_{b1} amplitude-distance curve for zero-depth events is fitted to the data in three different distance intervals. Information about the m_{b1} curve offset, the standard deviation, and the number of events for the different distance ranges is given in the lower right boxes.

6.4.3 Improvements to the TROLL station, February 2013

During the first year of operation, relatively large diurnal, long-period oscillations were observed at TROLL (Schweitzer *et al.*, 2012), presumably caused by temperature variations within the protected dome. In addition, the gain setting of the Q330HR digitizer was observed to be too low for sufficient resolution of the high-frequencies. Consequently, the gain setting of the Q330HR digitizer was increased on 4 February 2013 by a factor of 20, and on 9 February 2013, the TROLL station was upgraded with additional thermal insulation. An additional low-gain data stream with a sampling rate of 40 Hz was retained by using the auxiliary 24-bit input and a gain factor of 1. Fig. 6.4.7 illustrates different steps of the thermal insulation procedures.



Fig. 6.4.7 Photos taken during the installation of additional thermal insulation at the TROLL station in February 2013.

Upper left: Q330HR digitizer and cables inside the station after the removal of the covering plastic dome.

Upper right: The thermal insulation to be placed around the steel casing covering the seismometer.

Lower left: The thermal insulation put in place.

Lower right: Job finished. To avoid heating from the sunlight, the plastic dome covering the station was painted white (it was previously orange) and the surrounding area was again covered with stones.

Fig. 6.4.8 shows 9 days of raw, long-period vertical-component data from two similar time periods of the year in 2012 and 2013. It can be clearly observed that the amplitude of the daily signal is significantly reduced during the entire time period in 2013, after the installation of additional thermal insulation. In order to rule out the potential influence of differences in the weather conditions, we show in Fig. 6.4.9 the corresponding temperature profiles at the TROLL station during these two time periods in 2012 and 2013. The temperature profiles are quite similar. We therefore conclude that the reduction in the daily amplitudes after the installation of additional thermal insulation, shown in Fig. 6.4.8, is not caused by smaller temperature variations in 2013 as compared with 2012.

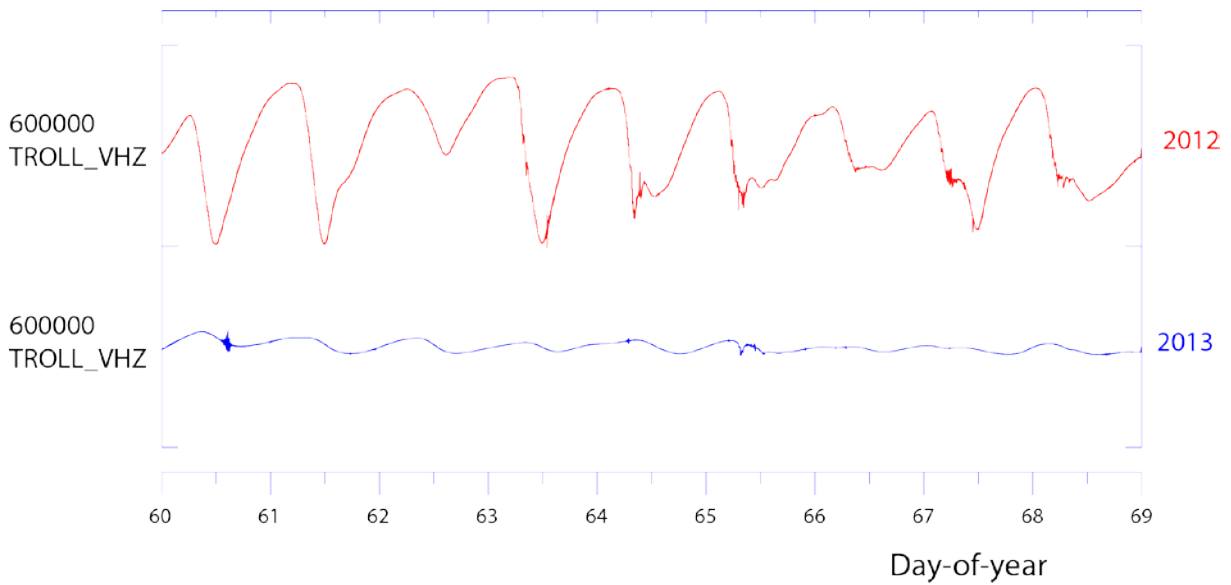


Fig. 6.4.8 Both traces show vertical-component seismograms for the TROLL VHZ channels. TROLL VHZ has a sampling rate of 0.1 Hz. Upper, red trace: 9 days of data starting on day-of-year 60 in 2012. Lower, blue trace: 9 days of data starting on day-of-year 60 in 2013, after the installation of additional thermal insulation.

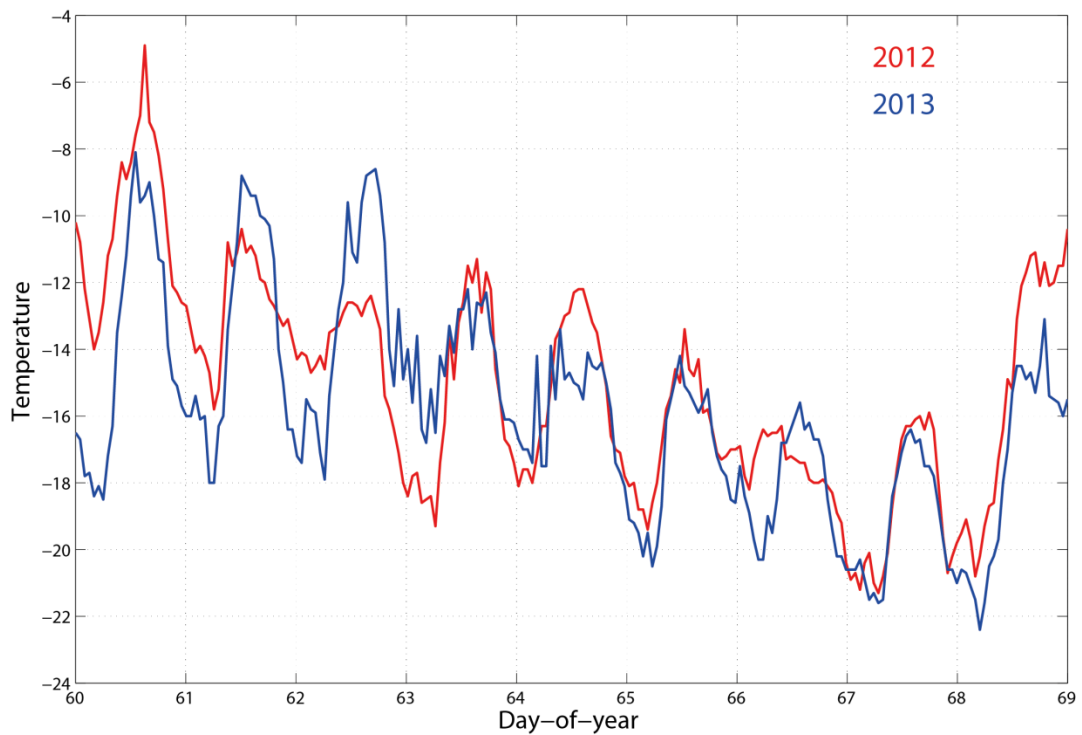
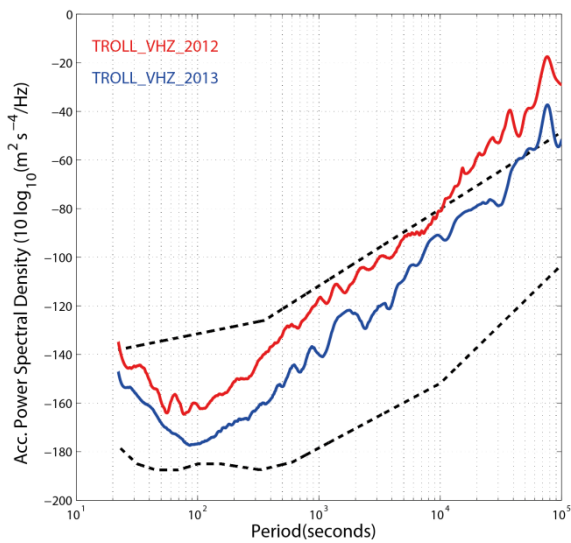
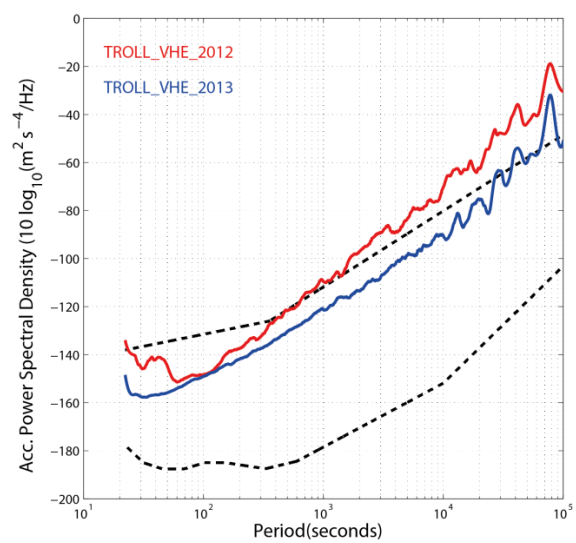
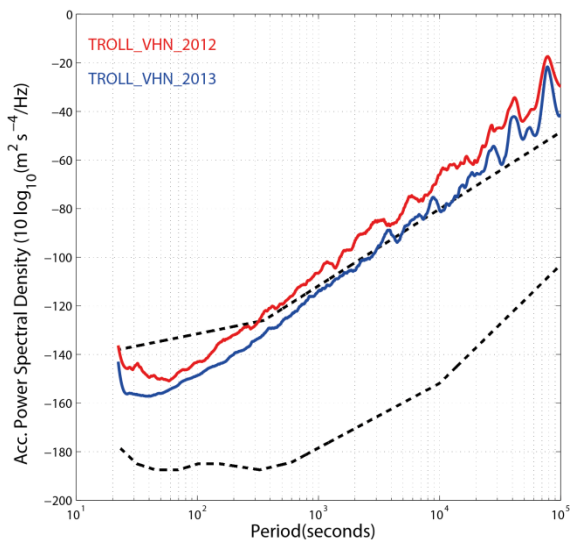


Fig. 6.4.9 Temperature profiles at TROLL for the two 9-day periods in 2012 and 2013. See Fig. 6.4.8 for details.

Fig. 6.4.10 shows the corresponding acceleration spectra for both the vertical and the horizontal components of the TROLL station. For the vertical component we observe in 2013 about 20 dB reduction for the diurnal period (86400 s). A similar improvement is also observed for periods between 100 and 3000 s. For 100 s period we observe in 2013 noise levels approaching the Peterson low-noise model on the vertical component. For the horizontal components, and in particular for the North-South component, the improvement is much smaller. It should also be noted that the long-period noise levels on the horizontal components are generally higher than on the vertical component (Peterson, 1993). We currently have the hypothesis that the thermal insulation may have been installed in such a way that it is slightly squeezed between the steel casing covering the seismometer and the covering plastic dome. This may explain the very small improvement in the north-south component noise levels, and we plan to investigate and, if necessary, correct this during the next summer season in January-February 2014.



*Fig. 6.4.10
TROLL acceleration spectra for the two 9-day time periods in March 2012 (red) and March 2013 (blue).
Left: Vertical component
Lower left: North-South component
Lower right: East-West component
The Peterson low- and high-noise models are shown as black dashed lines. Notice that the Peterson noise models are derived from long-period vertical component data, and may thus not be generally representative for the horizontal components.*



6.4.4 Observation of the Earth's normal modes with TROLL

Each strong seismic event (*i.e.*, with surface magnitudes above ~ 7) generates normal modes of the whole Earth. The largest Earth's normal mode period is 3233 s and many modes have periods between 500 and 1000 s. The generation of the different modes depends on the magnitude and double couple orientation of the event.

TROLL can record seismic energy with frequencies below 1 mHz (or periods above 1000 s), therefore it is of interest to investigate how well normal modes of the Earth can be observed at this new station. Since the installation of the station in February 2013, several earthquakes occurred, which were large enough to generate normal modes. In Fig. 6.4.11 we show spectra between 0.25 and 2.5 mHz of the vertical component after two such strong events. Unfortunately, none such strong events (here we used a threshold of $MS \geq 7.3$) occurred after improving the thermal insulation of the STS-2.5 in February 2013. Therefore, the effect of the lower, long period noise level (see Figs. 6.4.8 and 6.4.10) cannot be tested yet.

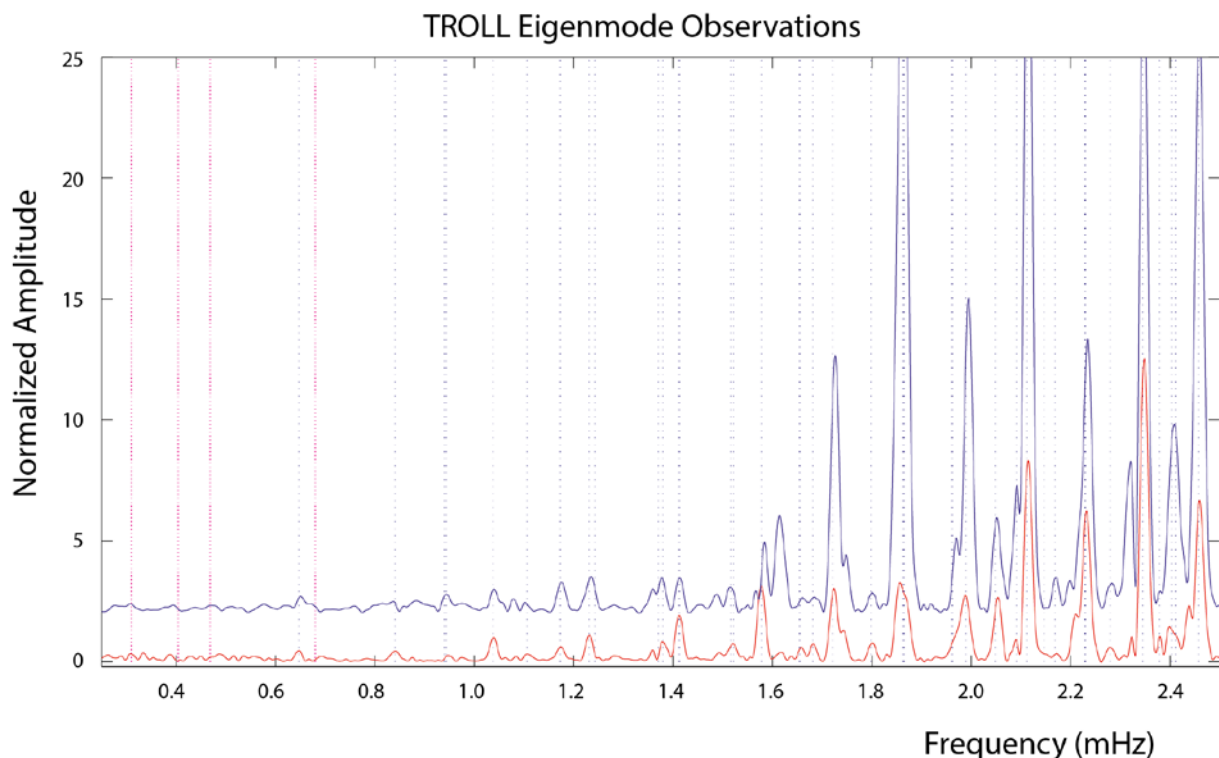


Fig. 6.4.11 Vertical component long-period spectra of 30 hour long TROLL data observed after the 11 April 2012 MS 8.5 Sumatra earthquake (blue) and the 6 February 2013 MS 7.4 Santa Cruz Islands earthquake (red). For more details see text.

To calculate the shown spectra, 30 hour long time windows starting at the event source time were bandpass filtered between 100 and 4000 s. Then, the seismic traces were tapered with a Hanning window and the spectra calculated with an FFT. The two data examples show normalized spectra for the 11 April 2012 MS 8.5 Sumatra earthquake (blue) and the 6 February 2013 MS 7.4 Santa Cruz Islands earthquake (red). Note that the blue spectrum has been offset vertically to improve its readability. Observable spheroidal normal mode frequencies (*e.g.*, Dziewonski and Anderson, 1981 or Deuss *et al.*, 2013) are indicated with dotted lines, with blue dotted lines indicating observed and magenta dotted lines non observed normal modes.

6.4.5 Conclusions

From the analysis of a 6 month dataset, we have shown that TROLL has an overall event detection capability which is 0.1 – 0.2 magnitude units better than SNAA for teleseismic events. Using the method of Kværna and Ringdal (2013) to estimate the overall detection capability of IMS stations, we show in Fig. 6.4.12 the offset of the best-fitting (m_{b1}) teleseismic detection capability curve for IMS auxiliary stations. These estimates are based on IDC REB data from the 11-year time period 1 January 2001 to 31 December 2011. As SNAA shows to be among the very best performing three-component stations of the IMS, TROLL is thus considered to be even better for detection of teleseismic events. The 1 – 2 Hz noise levels at SNAA and TROLL are comparable, but there is a tendency of higher noise levels at TROLL for higher frequencies, caused by *e.g.*, periodically occurring small icequakes in the nearby glaciers. This may influence the detection capability for regional and local events where high frequencies are dominant. Although located directly on bedrock with relatively little protection against environmental disturbances, the protection of the new station TROLL is good enough that the station can be used for studies of very long-period signals (normal modes of the Earth).

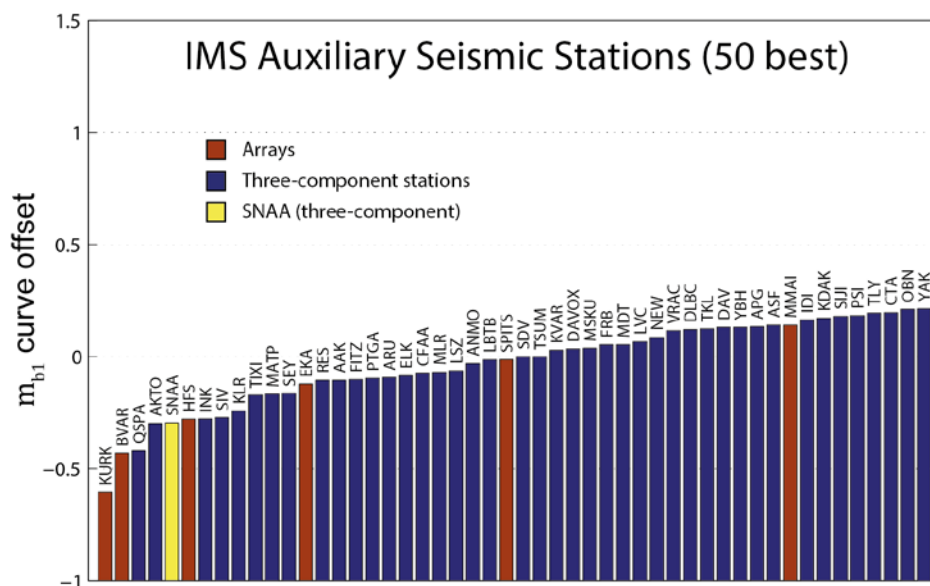


Fig. 6.4.12 Offset of the best-fitting m_{b1} detection capability curve for the 50 best IMS auxiliary stations for events in the teleseismic distance range 20 – 90°. Array stations are shown red and three-component stations are shown blue. SNAA is highlighted yellow.

The installation of additional thermal insulation at the TROLL station in February 2013 led to a significant reduction of the long period noise levels of the vertical component data. For the horizontal component the improvements are less significant, and we plan to have the TROLL site revisited during the austral summer season in January-February 2014 to check out if there are ways to further reduce the noise levels at horizontal components.

Acknowledgements

The TROLL project was financed by the Norwegian Polar Institute through its Norwegian Antarctic Research Expedition (NARE) program 2011 – 2014. In particular, we thank the staff of the Norwegian Antarctic research station Troll, who carried out the maintenance and refurbishment work in February 2013.

T. Kværna

J. Schweitzer

M. Pirli

M. Roth

References

Deuss, A., J. Ritsema and H. van Heijst (2013). A new catalogue of normal mode splitting function measurements up to 10 mHz. *Geoph. J. Int.*, **193**, 920-937.

Dziewonski, A.M. and D.L. Anderson (1981). Preliminary Reference Earth Model. *Phys. Earth Planet. Int.*, **25**, 1271-1302.

Kværna, T. and F. Ringdal (2013). Detection capability of the seismic network of the International Monitoring System for the Comprehensive Nuclear-Test-Ban Treaty. *Bull. Seism. Soc. Am.*, **103**, (2A), 759-772.

Peterson, J. (1993). Observations and modeling of seismic background noise. *USGS Open-File Report 93-322*, 95 pp.

Pirli, M. (2012). First Data and Analysis Results from the New, Permanent Seismic Station TROLL, Dronning Maud Land, Antarctica. *NORSAR Sci. Rep.*, **1-2012**, Kjeller, Norway, 47-55.

Schweitzer, J., M. Roth and M. Pirli (2012). The new three-component broadband station at Troll, Antarctica. *NORSAR Sci. Rep.*, **1-2012**, Kjeller, Norway, 39-46.